Neutrinos
their
Oscillations, Experiments
and
Unification with the Standard Model

A Term Paper submitted for the completion of
requirements for the course on

The Standard Model of Particle Phyiscs
HE 397

by

aman Sahoo, Neha, Nikshay Chugh
Center for High Energy Physics
Indian Institute of Science

Under the supervision of

Prof. B. Ananthanarayan
Center for High Energy Physics, Indian Institute of Science

Acknowledgements

This report has been compiled out under the guidance of **Prof. B. Ananthanarayan**, Center For High Energy Physics, Indian Institute of Science. We owe our deepest sense of gratitude to him for his continuous encouragement and expert suggestions, which gave us the inspiration to learn more. We thank him profoundly for his consistent support, perseverance and able guidance. His strictness full of benevolence and constructive criticism coupled with befitting counsels and patience paved the way for successful completion of this report/presentation. Under his supervision it has indeed been a pleasant privilege and a great experience..

Abstract

This report presents a comprehensive exploration of neutrino physics, tracing the historical development, theoretical foundations, and experimental discoveries that have shaped our current understanding of these elusive particles. Beginning with the historical puzzle of β-decay spectra, the narrative follows the theoretical proposal and eventual detection of the neutrino, establishing its central role in the Standard Model and beyond.

The phenomenon of neutrino oscillations is introduced through the lens of mass-induced flavor mixing, culminating in the formalism of the PMNS matrix and the inclusion of matter effects. Theoretical extensions beyond the Standard Model are discussed, focusing on the challenges of incorporating neutrino masses while preserving gauge invariance. Various sterile neutrino frameworks are systematically analyzed, including their Lagrangian formulations, mass generation mechanisms, and phenomenological consequences across distinct mass regimes.

Gauge invariance constraints, anomaly cancellation via $B-L$ symmetries, and the role of effective field theories are addressed to contextualize neutrino masses within a broader ultraviolet-complete framework. The report then delves into the seesaw mechanisms (Types I, II, and III), providing detailed mass matrix formulations and effective operator treatments. Connections to Grand Unified Theories, particularly within SO(10), are outlined as natural high-scale embeddings.

On the experimental front, the historical milestones in neutrino discovery are revisited, followed by a critical review of oscillation experiments, cosmological constraints from Big Bang Nucleosynthesis and Z boson decay, and direct searches for sterile neutrinos. The prospect of neutrinoless double-β decay is discussed as a potential probe of Majorana nature and lepton number violation.

Together, these elements provide a cohesive synthesis of theoretical models and experimental strategies aimed at deciphering the fundamental properties of neutrinos and their implications for particle physics and cosmology.

Contributions: Parts 1 and 2 were done by Neha. Part 3 was done by Nikshay. Parts 4 and 5 were done by Aman.

Contents

Part I

Introduction

Chapter 1

A Little Bit of History

In 1911 and later in 1914, James Chadwick observed that the β-decay spectrum of radioactive elements was continuous, unlike the discrete spectra of α- or γ-radiation . This puzzling result implied that some energy was missing, suggesting the existence of an undetected particle carrying away that energy.

In 1930, Wolfgang Pauli proposed a bold solution to this mystery. He suggested the existence of a new, neutral, weakly interacting particle with spin-½ and a mass comparable to the electron. Initially, in analogy with the proton, Pauli referred to this hypothetical particle as the neutron . However, in 1932, Chadwick discovered a much more massive neutral particle—strongly interacting and similar in mass to the proton—which rightly took the name neutron .

To avoid confusion, Enrico Fermi coined the term neutrino (Italian for "little neutral one") for Pauli's proposed particle and incorporated it into his revolutionary theory of β-decay published in 1934 . Fermi's theory successfully explained β-decay and lent strong theoretical support to the existence of neutrinos. Yet, the particle remained undetected for decades. Even Pauli himself worried that he might have postulated a particle that could never be observed.

However, progress in nuclear fission research during the 1930s and 1940s provided an intense and steady source of antineutrinos, opening the door to potential experimental detection. In the early 1950s, inspired by Bruno Pontecorvo, Frederick Reines and Clyde L. Cowan Jr. designed an experiment at the Savannah River nuclear reactor in South Carolina. They sought to detect antineutrinos via their interactions with protons in a detector medium—specifically, through the process known as inverse -decay. In this reaction, an antineutrino interacts with a proton, producing a neutron and a positron, both of which could be detected.

In June 1956, Reines and Cowan achieved success: they provided the first direct experimental evidence for the existence of neutrinos. Just two years before Pauli's death, they sent him a telegram informing him of the discovery. Their results, confirming Pauli's hypothesis, were published in Science in July 1956 . For this landmark achievement, Reines was awarded the Nobel Prize in Physics in 1995, which he shared with Martin L. Perl.

Part II

Neutrino Oscillations

Chapter 2

Neutrinos with Mass

Helicity is a meaningful label for massless particles because all observers, regardless of their frame of reference, agree on its value. If neutrinos have mass.In that case, helicity is no longer a good quantum number, because Lorentz boosts can flip the helicity for massive particles.Therefore, massive spin-½ particles are labeled by their rest-frame spin, $\sigma = \pm\frac{1}{2}$, rather than helicity. A generic state is written as $|\nu_i(p,\sigma)\rangle$. Applying CPT flips the spin direction , but since the particle already has both spin eigenvalues, it is no longer guaranteed that the CPT-conjugate state is distinct.

- If there exists a conserved quantum number—such as lepton number—that distinguishes the neutrino from its CPT-conjugate, the neutrino is called a Dirac neutrino. $|\nu_i\rangle \neq \text{CPT}|\nu_i\rangle$
- If no such conserved quantum number exists, the neutrino is a Majorana neutrino, meaning the CPT conjugate of the state is identical to the state itself $|\nu_i\rangle = \text{CPT}|\nu_i\rangle$

The terms Dirac and Majorana arise from the corresponding field representations.For any spin-½ particle, the minimal two states—$|\nu(p,\sigma)\rangle$ and its CPT-conjugate $|\bar{\nu}(p,-\sigma)\rangle$ can be described by a Majorana spinor.A collection of NN such particles can therefore be described by N Majorana fields.
However, if the theory possesses a global U(1) symmetry , it becomes convenient to pair two Majorana spinors—ψ_1 and ψ_2—into a Dirac spinor.

$$\psi_D = P_L\psi_1 + P_R\psi_2, \tag{2.1}$$

with U(1) acting as $\psi_D \to e^{i\alpha}\psi_D$
In the Standard Model, this Dirac construction is applied to all fermions except neutrinos, because the other fermions carry electric charge, which clearly distinguishes particles from antiparticles. Since neutrinos are neutral , their particle/antiparticle distinction hinges solely on whether lepton number is conserved.Although neutrino oscillation experiments demonstrate that individual lepton numbers are not conserved, they do not definitively answer whether total lepton number is conserved. [1]

Chapter 3

Neutrino Oscillations

A key decision in modeling neutrino oscillations is whether to introduce additional neutrino species beyond the three known flavors. As we shall see, reintroduce gauge invariance ultimately connects this choice to the question of whether to extend the Standard Model by introducing new particles or non-renormalizable interaction.

3.1 Three Neutrinos

Suppose there are no additional neutrino states beyond the Standard Model. Then, CPT symmetry ensures neutrinos are their own antiparticles.This condition rules out the possibility of lepton number being even approximately conserved. Consequently, any neutrino mass terms in this scenario necessarily violate total lepton number L, as well as the individual flavor lepton numbers Le, $L\mu$, and $L\tau$ To describe neutrino masses phenomenologically, the Standard Model Lagrangian is modified:

$$\mathcal{L} = \mathcal{L}_{SM} - \frac{1}{2}\left[m_{ij}(\bar{\nu}_i P_L \nu_j) + \text{c.c.}\right] \tag{3.1}$$

where m_{ij} is a complex symmetric 3×3 matrix.
This mass term differs significantly from the Dirac-type mass terms associated with quarks and charged leptons, which connect left- and right-handed fields. In contrast, the Majorana mass term couples a field to itself.
Expressed in terms of the two-component left-handed spinor χ, where the Majorana spinor is written as $\nu = [\chi \epsilon \chi *]^T$, the mass term becomes:

$$\mathcal{L}_{\nu,\text{mass}} = \frac{1}{2}\left[m^*_{ij}\chi_i^T \chi_j + \text{h.c.}\right] \tag{3.2}$$

Such a term, which couples a field to its own transpose rather than to an independent right-handed field, is referred to as a Majorana mass. The Majorana mass term breaks all global lepton number symmetries of the Standard Model. Under lepton flavor rotations, the left-handed fields transform as $P_L\nu_j \to e^{i\omega_j} P_L \nu_j$where each flavor has an independent phase ω_j
The mass matrix takes the form

$$m_{jk} \to m_{jk} e^{i(\omega_j + \omega_k)} \tag{3.3}$$

This transformation shows that the mass term is invariant under lepton number rotations.It is invariant under all three transformations only if $m_{jk} = 0$. The same is also true for the overall lepton symmetry, for which $\omega_1 = \omega_2 = \omega_3 = 0$. The only type of lepton number which Eq. can preserve is the difference between two lepton numbers; e.g. $L_{12} = L_1 - L_2$ would be a symmetry if the only nonzero mass matrix elements were m_{33} and $m_{12} = m_{21}$. In such a case the neutrinos ν_1 and ν_2 would group into a Dirac neutrino .With the third neutrino being necessarily Majorana if $m_{33} = 0$.

3.2 The PMNS Matrix

After transforming to the neutrino mass basis, the neutrino part of the Lagrangian becomes

$$\mathcal{L} = -\frac{1}{2}\bar{\nu}_i \left(\not{\partial} + m_i \right) \nu_i + \mathcal{L}_{\rm nc} + \mathcal{L}_{\rm cc} \tag{3.4}$$

$\mathcal{L}_{nc}$ is unchanged from the standard model and the charged-current interaction picks up a CKM-like mixing matrix,

$$\mathcal{L}_{\rm cc} = \frac{igV_{ai}}{\sqrt{2}} W_\mu \left(\bar{\ell}_a \gamma^\mu \gamma_L \nu_i \right) + \text{h.c.} \tag{3.5}$$

Neutrino flavor states $|\nu_\alpha\rangle$ related with mass states $|\nu_i\rangle$ by PMNS matrix V where V=UK with $K = Diag(e^{i\frac{\alpha_1}{2}}, e^{i\frac{\alpha_2}{2}}, e^{i\frac{\alpha_3}{2}})$

$$U = \begin{bmatrix} c_{12}c_{13} & s_{12}c_{13} & s_{13}e^{-i\delta} \\ -s_{12}c_{23} - c_{12}s_{23}s_{13}e^{i\delta} & c_{12}c_{23} - s_{12}s_{23}s_{13}e^{i\delta} & s_{23}c_{13} \\ s_{12}s_{23} - c_{12}c_{23}s_{13}e^{i\delta} & -c_{12}s_{23} - s_{12}c_{23}s_{13}e^{i\delta} & c_{23}c_{13} \end{bmatrix} \tag{3.6}$$

The matrices U and V differ because of the appearance of the extra phases, α_i, in the matrix K. Such phases are removed in CKM matrix by performing phase rotations of the first- and second-generation quarks.The same rotations also would have removed the phases $e^{i\alpha j}$ if neutrinos had been Dirac particles. One of the phases α_i can be rotated away by making a common phase rotation of the charged leptons and the other two are not observable in processes which conserve total lepton number L.
The probability of the neutrino being produced as flavor eigenstate ν_a and being detected in flavor eigenstate ν_b is

$$P_{\nu_a \to \nu_b}(E, L) = |\langle \nu_b(L,t) | \nu_a(0,0) \rangle|^2 = \sum_{i,j} e^{-i\frac{(m_i^2 - m_j^2)L}{2E}} U_{bi} U_{bj}^* U_{aj} U_{ai}^* \tag{3.7}$$

Mass squared differences: $\Delta m_{ij}^2 = m_i^2 - m_j^2$; Mixing angles: $\theta_{12}, \theta_{13}, \theta_{23}$; CP-violating phase: δ

Two-flavor approximation:

$$P(\nu_\alpha \to \nu_\beta) = \sin^2(2\theta)\sin^2\left(\frac{\Delta m^2 L}{4E}\right) \tag{3.8}$$

[2]

3.3 Matter Effect on Neutrino Oscillation

Neutrino experiments often involve detecting neutrinos that originate at a source on the earth's surface, travel through the bulk material of the earth and get detected at a detector placed on the surface several kilometres away. In such cases, we need to consider matter effects as well.

- Interaction with matter may cause a flavour change in a neutrino. But the Standard Model predicts that all neutrino-matter interactions are flavour conserving. Hence we do not consider this possibility
- Neutrinos can undergo forward scattering while interacting with particles, which will give rise to an extra interaction potential energy.

Charged current interaction (via W boson exchange) affects only ν_e:

$$V_W = \pm\sqrt{2}G_F N_e \tag{3.9}$$

Neutral current interaction (via Z boson exchange) affects all flavours equally:

$$V_Z = \mp\frac{\sqrt{2}}{2}G_F N_n \tag{3.10}$$

From mass eigenstates:

$$\mathcal{H}_{\text{Vac}} = \sum_i U^*_{\alpha i} U_{\beta i} E_i \tag{3.11}$$

Using the relativistic approximation,

$$\mathcal{H}_{\text{Vac}} = \frac{\Delta m^2}{4p}\begin{bmatrix} -\cos 2\theta & \sin 2\theta \\ \sin 2\theta & \cos 2\theta \end{bmatrix} + \left(p + \frac{m_1^2 + m_2^2}{4p}\right)\begin{bmatrix} 1 & 0 \\ 0 & 1 \end{bmatrix} \tag{3.12}$$

For a highly relativistic neutrino, the second term vanishes

$$\mathcal{H}_M = \mathcal{H}_{\text{Vac}} + V_W \begin{bmatrix} 1 & 0 \\ 0 & 0 \end{bmatrix} + (V_Z)\begin{bmatrix} 1 & 0 \\ 0 & 1 \end{bmatrix} \tag{3.13}$$

$$\mathcal{H}_M = \mathcal{H}_{\text{Vac}} + V_W \begin{bmatrix} 1 & 0 \\ 0 & -1 \end{bmatrix} + (V_W + V_Z)\begin{bmatrix} 1 & 0 \\ 0 & 1 \end{bmatrix} \tag{3.14}$$

Substituting $V_W = 2\sqrt{2}G_F N_e E/\Delta m^2$:

$$\mathcal{H}_M = \frac{\Delta m^2}{4E}\begin{bmatrix} -\cos 2\theta + x & \sin 2\theta \\ \sin 2\theta & \cos 2\theta - x \end{bmatrix} \tag{3.15}$$

where $x = 2\sqrt{2}G_F N_e E/\Delta m^2$
This can be interpreted as a change in $\theta \to \theta_M$ and $m \to m_M$

$$\sin^2 2\theta_M = \frac{\sin^2 2\theta}{\sin^2 2\theta + (\cos 2\theta - x)^2} \tag{3.16}$$

$$\Delta m^2_M = \Delta m^2 \sqrt{\sin^2 2\theta + (\cos 2\theta - x)^2} \tag{3.17}$$

resulting

$$\mathcal{H}_M = \frac{\Delta m^2_M}{4E}\begin{bmatrix} -\cos 2\theta_M & \sin 2\theta_M \\ \sin 2\theta_M & \cos 2\theta_M \end{bmatrix} \tag{3.18}$$

the eigenstates in matter:

$$|\nu_e\rangle = |\nu_1\rangle \cos\theta_M + |\nu_2\rangle \sin\theta_M, \tag{3.19}$$

$$|\nu_\mu\rangle = -|\nu_1\rangle \sin\theta_M + |\nu_2\rangle \cos\theta_M. \tag{3.20}$$

Eigenvalues of $\mathcal{H}_M$:

$$\lambda_1 = +\frac{\Delta m^2_M}{4E}, \quad \lambda_2 = -\frac{\Delta m^2_M}{4E}. \tag{3.21}$$

computing $P_M(\nu_e \to \nu_\mu)$:

$$P_M(\nu_e \to \nu_\mu) = \sin^2 2\theta_M \sin^2\left(\frac{\Delta m^2_M L}{4E}\right). \tag{3.22}$$

Replacing $\Delta m^2_M, \theta_M$ with $\Delta m^2, \theta$ we will get the vacuum case Matter effects depend on x:

$$|x| \approx \frac{E}{10.53\ \text{GeV}}. \tag{3.23}$$

Higher energy implies stronger matter effects
Estimate for x $\Delta m^2 = 2.4 \times 10^{-3}\ \text{eV}^2$ Fermi constant: $1.67 \times 10^{-23}\ \text{eV}^{-2}$ Mantle density: $3000\ \text{kg/m}^3$ $N_e = 6.89 \times 10^9\ \text{eV}^3$

$$|x| = 9.50 \times 10^{-11} E\ \text{eV}^{-1} \approx \frac{E}{10.53\ \text{GeV}}. \tag{3.24}$$

In special cases, matter effects can be dramatically large.
If $\theta \approx 0$, then $\sin^2 2\theta_M \approx 1$. Resonant amplification: $\theta_M \gg \theta$. [2]

Part III

Possible Theoretical Frameworks

Chapter 4

The Central Problem

4.1 What We Want

One of the most pressing shortcomings of the Standard Model (SM) of particle physics is its inability to account for the non-zero masses of neutrinos. Despite its immense success in describing the electromagnetic, weak, and strong interactions, the SM assumes that neutrinos are massless, which is now known to be inconsistent with experimental observations of neutrino oscillations. This necessitates theoretical extensions to the SM that can incorporate neutrino mass terms in a consistent and predictive manner.

Several theoretical approaches have been developed to explain neutrino masses. One class of models involves effective field theory, particularly through the inclusion of non-renormalizable operators. A prominent example is the dimension-five operator that extends the SM Lagrangian, often referred to as the νSM. Another approach introduces sterile neutrinos—right-handed neutrino fields that are singlets under the SM gauge group. These fields can mix with the active neutrinos and generate mass terms via interactions with the Higgs field or via explicit Majorana masses.

The seesaw mechanisms (Types I, II, and III) offer a compelling explanation for the smallness of neutrino masses by introducing heavy degrees of freedom that suppress the observed masses at low energies. In Type I seesaw, heavy right-handed Majorana neutrinos are introduced. Type II involves scalar triplets, and Type III includes fermionic triplets.

Beyond these, more unified frameworks have been proposed. Left-right symmetric models based on the extended gauge group $SU(2)_L \times SU(2)_R \times U(1)_{B-L}$ provide natural settings for right-handed neutrinos and may explain parity violation in weak interactions as a spontaneous symmetry breaking effect. Finally, Grand Unified Theories (GUTs), such as those based on the $SO(10)$ gauge group, naturally include right-handed neutrinos in their representations and predict neutrino masses as a consequence of unified symmetry breaking patterns.

The central theoretical question remains: why are neutrino masses so small compared to those of the charged fermions? Any successful framework must address this hierarchy in a natural and

consistent manner.

4.2 Gauge Invariance in Neutrino Models

In the Standard Model, gauge invariance plays a crucial role in determining the form of allowed interactions. The SM is based on the gauge group $SU(2)_L \times U(1)_Y$. The left-handed components of leptons and quarks transform as doublets under $SU(2)_L$, while the right-handed components are singlets. The Higgs field transforms as a doublet and is responsible for the generation of fermion masses via Yukawa couplings after spontaneous symmetry breaking.

However, the generation of neutrino masses within the SM is not straightforward. The standard model lacks right-handed neutrinos and hence does not allow for Dirac mass terms for neutrinos. To introduce neutrino masses, one must either add new degrees of freedom, such as right-handed neutrinos or scalar triplets, or relax the requirement of renormalizability by including higher-dimensional operators in the effective Lagrangian.

Chapter 5

Sterile Neutrinos

5.1 Lagrangian for Sterile Neutrinos

One of the most straightforward extensions of the SM is the addition of sterile neutrinos—fermions that do not participate in SM gauge interactions. These sterile neutrinos are often taken to be Majorana fields. Let us consider N such sterile neutrinos, labeled by s_x with $x = 1, \ldots, N$. These fields are SM singlets and can thus be introduced without violating gauge invariance.

The Lagrangian including these sterile neutrinos can be written as:

$$\mathcal{L} = \mathcal{L}_{\text{SM}} - \frac{1}{2} s_x \not{\partial} s_x - \frac{1}{2} \left(M_{xy} s_x P_L s_y + m_{ab} \nu_a P_L \nu_b + 2\mu_{ax} \nu_a P_L s_x + \text{c.c.} \right) \tag{5.1}$$

Here, m_{ab}, μ_{ax}, and M_{xy} are mass matrices characterizing the interactions among the active and sterile neutrinos. The term m_{ab} corresponds to Majorana mass terms for the active neutrinos, μ_{ax} describes the mixing between active and sterile states, and M_{xy} gives Majorana masses for the sterile neutrinos themselves.

The complete left-handed neutrino mass matrix in the basis (ν, s) is:

$$\begin{bmatrix} m & \mu \\ \mu^T & M \end{bmatrix} \tag{5.2}$$

This is an arbitrary complex symmetric matrix of dimension $(3 + N) \times (3 + N)$. The ability to choose the elements of m, μ, and M gives rise to a wide variety of models, each with different phenomenological implications.

5.2 Freedom in Neutrino Mass Choices

The freedom in selecting the structure of the mass matrices m, μ, and M provides a rich model-building arena. One particularly interesting possibility arises when the overall lepton number is conserved, which leads to purely Dirac mass terms. However, in more general scenarios, lepton

number may be violated either explicitly or spontaneously, leading to Majorana mass terms. These different scenarios will be discussed in greater detail in the following sections.

5.3 Dirac Neutrinos

If we assume that lepton number is a conserved symmetry, then the neutrinos must be Dirac particles. To realize this, we can introduce three sterile neutrino fields s_a with the same generation index as the active neutrinos. Under a global lepton number symmetry, these fields transform as:

$$P_L\nu_a \to e^{i\omega}P_L\nu_a, \quad P_L s_a \to e^{-i\omega}P_L s_a \tag{5.3}$$

To preserve this symmetry, the mass terms must satisfy the conditions:

$$m = M = 0 \tag{5.4}$$

In this case, the only non-zero term is μ_{ab}, which links the left-handed active neutrino with the right-handed sterile neutrino, thus forming a Dirac spinor:

$$\psi_a = P_L\nu_a + P_R s_a \tag{5.5}$$

Under the lepton number symmetry, this Dirac field transforms as $\psi_a \to e^{i\omega}\psi_a$. The masses of these Dirac neutrinos arise from the μ matrix, and their eigenvalues correspond to the square roots of the eigenvalues of $\mu\mu^\dagger$.

5.4 Yukawa Terms

An alternative route to generating neutrino masses involves the introduction of right-handed neutrinos N_m that are singlets under the SM gauge group and have zero hypercharge. This allows the construction of a gauge-invariant Lagrangian involving Yukawa interactions:

$$\mathcal{L}_N = -\frac{1}{2}\bar{N}_m \not{\partial} N_m - \frac{1}{2}M_m\bar{N}_m N_m - \left(k_{mn}\bar{L}_m P_R N_n\tilde{\phi} + \text{h.c.}\right) \tag{5.6}$$

Here, $\tilde{\phi}$ is the conjugate Higgs field, and k_{mn} are Yukawa coupling constants. The term $\bar{L}_m P_R N_n\tilde{\phi}$ represents the Yukawa interaction that couples the left-handed lepton doublets to the right-handed neutrinos.

5.5 Lepton Number Violation

In this framework, we can assign lepton number $L = +1$ to $P_R N$. The Yukawa interactions can potentially violate individual lepton flavors (i.e., L_e, L_μ, and L_τ) if the matrix k_{mn} is non-

diagonal. More importantly, the Majorana mass term:

$$M_m \bar{N}_m N_m \tag{5.7}$$

violates the total lepton number $L = L_e + L_\mu + L_\tau$ by two units, indicating that the resulting neutrinos are Majorana particles. This is the core feature of the seesaw mechanism.

5.6 Neutrino Masses from Yukawa Couplings

Upon electroweak symmetry breaking, the Higgs field acquires a vacuum expectation value (VEV), reducing the theory to an effective sterile-neutrino framework. The masses of the neutrinos are then given by:

$$m_{ab} = 0, \quad \mu_{ab} = k_{ab}\frac{v}{\sqrt{2}}, \quad M_{ab} = M_a \delta_{ab} \tag{5.8}$$

The Dirac mass μ_{xa} is on the order of the electroweak scale ($\sim$ 100 GeV), while the Majorana mass M_m can be at or above the weak scale. This hierarchy leads to the small masses of the light neutrinos via the seesaw mechanism.

5.7 Helicity Suppression in Neutrino Scattering

The detection and production of neutrinos are subject to helicity suppression. This means that the amplitude for producing or detecting a neutrino is proportional to a power of its small mass. Consider a process where a neutrino is produced at a source and detected at a distant detector. The transition amplitude is governed by the propagator:

$$M = \frac{G_F^2}{2} J^\mu_{\text{prod}} J^\nu_{\text{det}} \left[(\cdots)\gamma_\mu(1+\gamma_5)\frac{-i\not{k} + m}{k^2 + m^2}\gamma_\nu(1 \pm \gamma_5)(\cdots) \right] \tag{5.9}$$

The sign in the final vertex depends on the detection interaction, and the Dirac structure of the propagator determines which components of the neutrino field contribute.

Detection of the sterile component s_a requires projection using $(1-\gamma_5)$, while detection of the active component ν_a requires $(1+\gamma_5)$. Only the mass term m in the numerator contributes to the detection of the sterile component, whereas the kinetic term $\not{k}$ contributes to the detection of the active component.

As a result, the detection probability of sterile neutrinos is suppressed. The amplitude ratio between sterile and active detection is roughly k^0/m, and for MeV-scale neutrinos, this ratio becomes 10^{-6}, corresponding to a suppression factor of 10^{-12} in probability. Therefore, the impact of sterile neutrinos on conventional neutrino phenomenology is minimal.

5.8 Generic Sterile Neutrinos and Phenomenology

When considering generic sterile neutrinos, the diagonalization of both the neutrino and charged-lepton mass matrices leads to a rich and complex structure in the neutrino sector. The presence of additional sterile states modifies the Pontecorvo–Maki–Nakagawa–Sakata (PMNS) matrix, introducing new mixing angles and CP-violating phases. Furthermore, new neutral-current interactions can arise through extended mixing matrices, denoted as H_{uv} and H'_{uv}.

These extensions have observable consequences in neutrino oscillation experiments, especially if the sterile states have masses in the eV to keV range. However, current experimental data place stringent constraints on the parameters of these models. Theoretical efforts continue to explore four main regimes of sterile neutrino models, classified by the relative magnitudes of the mass matrix elements m_{ab}, μ_{ax}, and M_{xy}.

5.9 Neutrino Mass Regimes and Theoretical Interpretations

The nature of neutrino masses remains one of the central questions in particle physics. Various theoretical frameworks propose different regimes based on the relative sizes of three mass parameters: the Majorana mass of left-handed neutrinos m, the Dirac mass μ that couples active and sterile states, and the Majorana mass M of right-handed (sterile) neutrinos. Each hierarchy among these mass scales results in qualitatively distinct phenomenology, implications for neutrino oscillations, cosmology, and underlying symmetries. We explore these regimes in detail.

5.9.1 Regime 1: $\mu \ll m, M$

In the limit where the Dirac mass μ is much smaller than both the Majorana masses m and M, the sterile neutrinos essentially decouple from the active sector. Their mixing with the active neutrinos becomes negligible, and thus they do not significantly affect oscillation experiments. In this regime, standard model neutrinos are accurately described by the Majorana mass matrix m, implying that the mass eigenstates are predominantly composed of left-handed neutrino fields. Although sterile neutrinos are inert in laboratory oscillation experiments, they may still contribute to cosmological phenomena, for instance, through their possible role in early universe dynamics or dark matter content.

5.9.2 Regime 2: Pseudo-Dirac Neutrinos ($\mu \gg m, M$)

A drastically different scenario arises when the Dirac mass μ dominates over both m and M. In the extreme limit where $m = M = 0$, the neutrino mass matrix describes purely Dirac particles. For $N = 3$, this yields three Dirac neutrinos, while additional sterile, massless neutrino states

appear for $N > 3$. Upon including small perturbations m and M, each Dirac neutrino splits into a pair of nearly-degenerate Majorana states with maximal mixing, characteristic of the so-called pseudo-Dirac neutrinos. Oscillation effects between these states become significant over long baselines, with oscillation lengths given approximately by $L \approx \frac{2E}{\Delta m^2}$, where Δm^2 denotes the squared mass splitting between the pseudo-Dirac partners. However, stringent constraints from solar neutrino experiments require these splittings to be extremely small, imposing upper bounds such as $m, M \lesssim 10^{-9}$ eV, thereby tightly constraining the parameter space of this regime.

5.9.3 Regime 3: Light Sterile Neutrinos ($m \sim \mu \sim M$)

When all the mass parameters m, μ, and M are of similar magnitude, the resulting mass matrix leads to the presence of $(3+N)$ Majorana neutrino states. This situation implies that the sterile and active states are heavily mixed, and the full neutrino spectrum includes mass eigenstates with significant sterile components. For these states to account for observed oscillation data, their masses typically need to be around 10^{-2} eV. Such a scenario naturally leads to large oscillation effects due to the extensive mixing. However, no experimental evidence has yet confirmed the existence of such light sterile neutrinos. Nonetheless, certain theoretical models have been proposed which avoid the most stringent experimental constraints, keeping the possibility of this regime open.

5.9.4 Regime 4: Seesaw Neutrinos ($m \ll \mu \ll M$)

Perhaps the most theoretically compelling regime is realized when $m \ll \mu \ll M$. In this hierarchy, the mass matrix yields N heavy eigenstates, with masses primarily determined by the large Majorana scale M, and three light eigenstates whose masses are suppressed by the inverse of M, consistent with the seesaw formula. The heavy states are mostly sterile, with mixing angles of the order μ/M, indicating very weak interaction with standard model particles. The light eigenstates, in contrast, remain predominantly active neutrinos. This structure elegantly explains the smallness of observed neutrino masses through the seesaw mechanism, with mass scales of order $O(\mu^2/M)$, which can naturally fall in the sub-eV range even if μ is at the electroweak scale and M is at the GUT or intermediate scale. This scenario is also theoretically attractive as it fits neatly into the gauge framework of the Standard Model, particularly within the electroweak symmetry group $SU(2)_L \times U(1)_Y$.

Chapter 6

Implications of Gauge Invariance

Gauge invariance plays a crucial role in shaping the interactions and mass terms of neutrinos. It fundamentally explains why sterile neutrinos, being singlets under the Standard Model gauge group, do not couple directly to gauge bosons or standard matter. Furthermore, the observed mass hierarchy $m \ll \mu \ll M$ emerges naturally when considering gauge-invariant mass terms and Yukawa couplings. This gives theoretical justification to the seesaw mechanism, as it is compatible with the gauge structure and symmetry-breaking patterns of the Standard Model.

6.1 Challenges and Fine-Tuning Issues

Despite the conceptual appeal of the seesaw mechanism, the realization of small neutrino masses imposes severe constraints on Yukawa couplings. The trace of the neutrino Yukawa matrix must satisfy

$$\mathrm{Tr}(k_{mn}) < 4 \times 10^{-12}, \tag{6.1}$$

indicating extraordinarily small couplings, many orders of magnitude smaller than those of charged fermions. Moreover, if one postulates a Majorana mass M_m generated through some high-scale symmetry breaking, it must satisfy an even more stringent constraint,

$$M_m < 10^{-20}\mu, \tag{6.2}$$

posing the question of why the model should require such extreme fine-tuning. These challenges motivate the search for more fundamental symmetries or mechanisms that can naturally explain these hierarchies without invoking arbitrary suppression.

Chapter 7

$B - L$ Symmetry and Anomalies

An exact $B - L$ (baryon number minus lepton number) symmetry could enforce $M_m = 0$, thus eliminating Majorana masses at tree level. However, such an exact symmetry is in tension with several phenomenological requirements, including the explanation of the baryon asymmetry of the universe and the standard charge assignments needed to maintain neutron neutrality. If $M_m = 0$ strictly, then reproducing a neutral neutron in terms of constituent quark charges becomes difficult without further assumptions or fine-tuning. Therefore, while $B - L$ symmetry can be useful, it must be either spontaneously or softly broken in realistic models.

7.1 Gauge Extensions Involving $B - L$

In the Standard Model, $B - L$ is an accidental global symmetry. However, if one promotes it to a local gauge symmetry, then the gauge group becomes $SU(2)_L \times U(1)_Y \times U(1)_{B-L}$. In this extended framework, anomaly cancellation mandates the inclusion of right-handed neutrinos. Moreover, breaking $B - L$ at a high energy scale can be directly related to the origin of the Majorana mass term, thus connecting with the seesaw mechanism. Left-right symmetric models, with gauge group $SU(2)_L \times SU(2)_R \times U(1)_{B-L}$, offer another path toward understanding the parity violation observed in weak interactions. In such models, right-handed neutrinos are embedded in $SU(2)_R$ doublets, and the breaking of $B-L$ symmetry provides a natural origin for their Majorana masses. These extensions highlight how neutrino physics is intimately connected with deep questions about fundamental symmetries and the structure of the Standard Model itself.

Chapter 8

The νSM: Effective Field Theory Approach

An alternative framework to incorporate neutrino masses is the effective field theory (EFT) extension of the Standard Model, often referred to as the νSM. In this approach, one introduces non-renormalizable interactions suppressed by a high energy scale Λ, without the need to add new particles explicitly. EFTs are widely used in particle physics and assume that at low energies, the full theory can be approximated by a series expansion in terms of higher-dimension operators. Truncating this expansion at the lowest non-renormalizable level yields predictive power.

In the νSM, the leading such operator is dimension five. It is unique in being both gauge-invariant and Lorentz-scalar:

$$\mathcal{L}_{\text{eff}} = -\tilde{k}_{mn}\tilde{\phi}^{\alpha}(\bar{L}_m^{\alpha}P_R L_n^{\beta})\tilde{\phi}^{\beta} + \text{h.c.}, \tag{8.1}$$

where ϕ is the Higgs doublet, L_m are the lepton doublets, and $\tilde{k}_{mn} = c_{mn}/\Lambda$ encodes the suppression by a high-energy scale. This operator violates lepton number by two units ($\Delta L = 2$), and upon electroweak symmetry breaking, it leads to Majorana masses for neutrinos.

In the unitary gauge, the Higgs field takes the form $\phi \to (0, v + H)^T/\sqrt{2}$, leading to an effective mass term:

$$\mathcal{L}_{\text{eff}} = -\frac{1}{2}\tilde{k}_{mn}(\nu_m P_R \nu_n)(v + H)^2 + \text{h.c.}, \tag{8.2}$$

which, upon evaluating the VEV, gives neutrino masses

$$m_{ab} = \tilde{k}^*_{ab}v^2 = c^*_{ab}\frac{v^2}{\Lambda}. \tag{8.3}$$

Taking $m_\nu \sim 50$ meV as an observed value, this implies $\Lambda \sim 10^{14}$ GeV, close to the GUT scale. This result provides a compelling explanation for the smallness of neutrino masses without invoking unnaturally small parameters.

8.1 Possible Origins and Experimental Tests

The presence of the dimension-5 operator strongly suggests that the Standard Model is only an effective theory valid below some high scale. The full theory above this scale may involve new particles or symmetries that give rise to the operator upon integration out of heavy degrees of freedom. One significant experimental test of the νSM framework is the observation of lepton number violating processes. The most notable among them is neutrinoless double beta decay. A positive signal would confirm the Majorana nature of neutrinos.

Lepton flavor violation is another avenue, though so far only observed in neutrino oscillations. Other decay processes such as $\mu \to e\gamma$, $Z \to \ell\ell'$, or $h \to \ell\ell'$ are being searched for, though predictions within the νSM place them far below current experimental sensitivities.

Finally, the unitarity of the Pontecorvo-Maki-Nakagawa-Sakata (PMNS) matrix provides a crucial consistency check. The νSM assumes the PMNS matrix is 3×3 and unitary. Any experimental deviation would necessitate the existence of additional neutrinos or non-standard interactions.

8.2 The Λ Scale and Its Role

In all effective theories, the scale Λ suppresses the effects of higher-dimension operators. In the νSM, neutrino masses arise from dimension-five operators and thus are inversely proportional to Λ. For experiments with energies $E \ll \Lambda$, only the ratio $z\nu/\Lambda$ can be probed, meaning that precise measurements of neutrino masses indirectly inform us about the scale of new physics. Understanding the value of Λ is critical to connecting low-energy neutrino data with high-energy theories, such as grand unification or string theory.

8.3 Motivation from the Ultraviolet Behavior of the Standard Model

The Standard Model (SM) of particle physics, though remarkably successful in describing phenomena up to the electroweak scale, is widely understood to be an effective theory, valid only below a certain ultraviolet (UV) cutoff scale Λ. Given the non-renormalizability of gravity and the emergence of quantum gravitational effects at the Planck scale, it is evident that $\Lambda \ll M_{\rm Pl} \sim 10^{19}$ GeV. This limitation necessitates the exploration of new physics beyond the SM, particularly to account for phenomena such as neutrino masses, which are experimentally verified but not accommodated in the original SM framework.

8.4 Dimensional Estimates and the Planck Scale

From dimensional analysis, one can anticipate that the masses of particles generated by higher-dimensional operators suppressed by the Planck scale would be on the order of

$$m_i \gtrsim \frac{v^2}{M_{\rm Pl}}, \tag{8.4}$$

where $v \approx 246$ GeV is the vacuum expectation value (VEV) of the Higgs field. This estimation yields $m_i \sim 10^{-5}$ eV, intriguingly close to the experimentally observed values of neutrino masses, suggesting a natural connection between the lightness of neutrinos and physics at high scales.

8.5 Grand Unified Scale and Neutrino Masses

If dimension-5 operators responsible for neutrino masses originate at a Grand Unified Theory (GUT) scale $\Lambda_{\rm GUT} \approx 10^{16}$ GeV, and the relevant Wilson coefficient z_ν is of order unity, then the generated neutrino mass is expected to be

$$m_\nu \approx \frac{v^2}{\Lambda_{\rm GUT}} \sim 10^{-2}\,{\rm eV}, \tag{8.5}$$

which is again compatible with experimental findings.

8.6 Upper Bounds on the New Physics Scale

Assuming $z_\nu \lesssim 1$, one obtains an upper bound on the scale Λ:

$$\Lambda \lesssim \frac{v^2}{m_\nu} \sim 10^{15}\,{\rm GeV}, \tag{8.6}$$

which is intriguingly close to the GUT scale.

Chapter 9

Seesaw Mechanisms for Neutrino Mass Generation

9.1 Type I Seesaw Mechanism

9.1.1 Field Content and Lagrangian

In the Type I seesaw, one introduces heavy gauge-singlet fermions N_m. The extended Lagrangian is:

$$\mathcal{L}_N = -\frac{1}{2}\bar{N}_m \partial\!\!\!/ N_m - \frac{1}{2} M_{mn} \bar{N}_m N_n - \left(k_{mn} \bar{L}_m P_R N_n \tilde{\phi} + \text{h.c.} \right), \tag{9.1}$$

where $\tilde{\phi} = i\tau_2 \phi^*$.

9.1.2 Light Neutrino Masses from the Seesaw

When $M \gg v$, the seesaw mechanism gives:

$$m_\nu \sim \frac{v^2}{M}. \tag{9.2}$$

9.1.3 Effective Operator after Integrating Out Heavy Neutrinos

The leading dimension-5 operator is:

$$\mathcal{L}_{\text{eff}} = -\left(k M^{-1} k^T \right)_{mn} \tilde{\phi}^\alpha \bar{L}_m P_R L_n \tilde{\phi}_\beta + \text{h.c.}, \tag{9.3}$$

with coefficient

$$\tilde{k}_{mn} = -\left(k M^{-1} k^T \right)_{mn}. \tag{9.4}$$

9.1.4 Mass Matrix Formulation

With Dirac and Majorana masses:

$$\mathcal{L}_N = -\bar{L} Y_\nu \tilde{\phi} N_R - \frac{1}{2} \bar{N}_R^c M_R N_R + \text{h.c.}, \tag{9.5}$$

leading to the mass matrix:

$$\mathcal{M} = \begin{pmatrix} 0 & m_D \\ m_D^T & M_R \end{pmatrix}, \quad m_D = Y_\nu \frac{v}{\sqrt{2}}. \tag{9.6}$$

For $M_R \gg m_D$:

$$m_\nu \approx -m_D M_R^{-1} m_D^T. \tag{9.7}$$

9.2 Type II Seesaw Mechanism

9.2.1 Scalar Triplet and Lagrangian

A scalar triplet $\Delta \sim (1, 3, -1)$ is introduced:

$$\mathcal{L}_\Delta = -(D_\mu \Delta)^\dagger D^\mu \Delta - M_\Delta^2 \Delta^\dagger \Delta - y_{mn} \bar{L}_m (\Delta \tau^a \mathcal{C}) P_R L_n + \text{h.c.}, \tag{9.8}$$

9.2.2 Effective Operator from the Triplet

Integrating out Δ yields:

$$\mathcal{L}_{\text{eff}} = -\frac{2 y_{mn} c}{M_\Delta^2} \tilde{\phi}^\alpha \bar{L}_m P_R L_n \tilde{\phi}_\beta + \text{h.c.} \tag{9.9}$$

9.2.3 VEV Induced Neutrino Mass

Alternatively, the triplet $\Delta \sim (1, 3, +2)$ couples via:

$$\mathcal{L}_\Delta = Y_\Delta \bar{L}^c i\tau_2 \Delta L + \text{h.c.}, \tag{9.10}$$

and gives

$$m_\nu = 2 Y_\Delta v_\Delta, \tag{9.11}$$

where

$$v_\Delta \sim \frac{\mu v^2}{M_\Delta^2}. \tag{9.12}$$

9.3 Type III Seesaw Mechanism

9.3.1 Fermionic Triplets and Lagrangian

Introduce $\Sigma \sim (1, 3, 0)$:

$$\mathcal{L}_\Sigma = -\bar{L} Y_\Sigma \tilde{\phi} \Sigma - \frac{1}{2} \mathrm{Tr}(\bar{\Sigma}^c M_\Sigma \Sigma) + \text{h.c.} \tag{9.13}$$

9.3.2 Resulting Neutrino Masses

Integrating out Σ gives:

$$m_\nu \approx -m_D M_\Sigma^{-1} m_D^T. \tag{9.14}$$

9.3.3 Phenomenology of Triplet Fermions

The triplet nature introduces charged partners, testable at colliders.

Chapter 10

GUT Embedding and High-Scale Physics

10.1 Seesaw in SO(10) GUTs

Grand Unified Theories, such as $SO(10)$, provide a framework in which all Standard Model gauge groups are unified into a single larger group. Within an $SO(10)$ GUT, one generation of fermions, including a right-handed neutrino, is embedded into a single 16-dimensional spinor representation. The seesaw mechanism is thus predicted naturally, and the relation

$$m_\nu \sim \frac{m_D^2}{M_R} \sim \frac{m_f^2}{M_{\mathrm{GUT}}} \tag{10.1}$$

emerges, explaining the vast disparity between the light neutrino masses and the masses of other fermions. In addition, such theories often link neutrino physics with the mechanism of leptogenesis, thereby providing a plausible explanation for the observed baryon asymmetry of the universe.

Part IV

Experiments and Observations

Chapter 11

Discovery of the neutrinos

11.1 ν_e neutrinos

Initially hypothesized to preserve the conservation laws governing β-decay in atomic nuclei, the electron neutrino(or rather antineutrino) was first detected in the Cowan-Reines neutrino experiment. [3] With the principal reaction

$$\bar{\nu_e} + p \rightarrow n + e^+ \tag{11.1}$$

having a total cross section of $6 \times 10^{-44} cm^2$, the experiment warranted the use of 2 tanks (total volume 200 L spiked with 40 kg of $CdCl_2$) sandwiched between between three scintillator layers which contained 110 five-inch photomultiplier tubes. The source of (anti-)neutrinos was a nuclear reactor with a neutrino flux of $5 \times 10^{13} s^{-1} cm^{-2}$, produced from β^- decay of the form

$$^{131}_{53}\mathrm{I} \rightarrow {}^{131}_{54}\mathrm{Xe}^* + \beta^- + \bar{\nu}_e + 606\,\mathrm{keV} \tag{11.2}$$

The neutrinos interaction with water's nuclei (Hydrogen), produces an easily recognizable signal. The e^+, quickly annihilates with any nearby e^-. The two resulting coincident γ are detected by the scintillator. The neutron can be detected by its capture by an appropriate nucleus $\mathrm{n} + {}^{108}\mathrm{Cd} \rightarrow {}^{109}\mathrm{Cd} + \gamma$, releasing a third gamma ray. The coincidence of the positron annihilation and neutron capture events gives a unique signature of an antineutrino interaction.

11.2 ν_μ neutrinos

In 1937 muons had been discovered in cosmic rays and this opened a route to the second neutrino flavor. When in 1948 the electron spectrum from muon decay was found to be continuous it was concluded that two neutrinos are emitted along with the electron. The Alternating Gradient Synchrotron (AGS), with its strong focusing ability, allowed high energy proton-nucleon collisions, resulting in pions that could decay into a beam of neutrinos. The steel and concrete

shielding (between the accelerator and the spark chamber) took advantage of the different decay times (Fig) to allow only the neutrinos generated by pion decay to pass through. A small fraction of the neutrinos would then get captured by the nucleons in the spark chamber giving rise to a reaction of the type

$$\nu_l + n \rightarrow p + l^- \tag{11.3}$$

where l^- would stand for either electron or a muon, with the estimated cross section of some $10^{-38} cm^2$ at 1 GeV[4] All 29 events recorded by the spark chamber indicated the passage of muons, indicating a 2^{nd} generation of neutrinos distinct from the ν produced in β-decay.

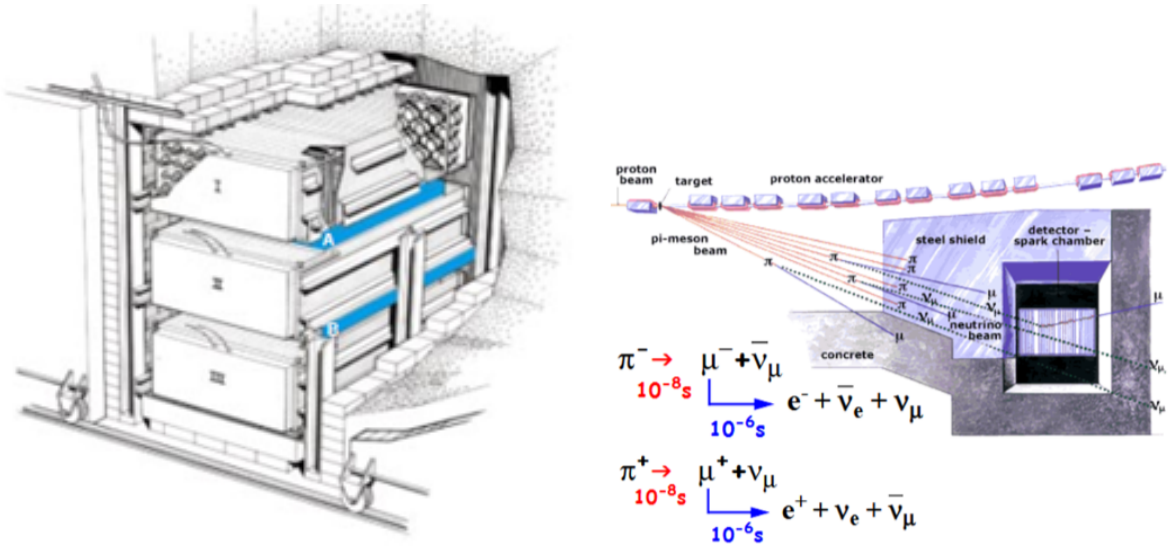

(a) (b)

Figure 11.1: (a)Cowan Reines Detector Setup (b) Alternate Gradient Synchrotron

11.3 ν_τ neutrinos

After the discovery of the tau lepton and t-quark (1977 and 1995, resp.), the hunt began for the tau neutrino, now that a third quark and lepton had been firmly established. The Direct Observation of NU Tau (DONUT) collaboration exposed sophisticated nuclear emulsion targets to the intense beam of neutrinos created by bombarding a Tungsten target with the 800 GeV proton beam at the Tevatron. [5]

The neutrino beam by assumption contained some 10% of tau neutrinos, originating mostly from the decay of the heavy D_s ($c\bar{s}$) meson. The tau neutrino would upon interaction (similar to eq.(36)) in the steel plate to produce a tau lepton. At its short lifetime the τ would at most cover a couple of millimeters before decaying into either an electron, a muon, or a hadron, and the neutrinos. The τ which would reach the emulsion would leave a short track extending into a long track after a characteristic kink.

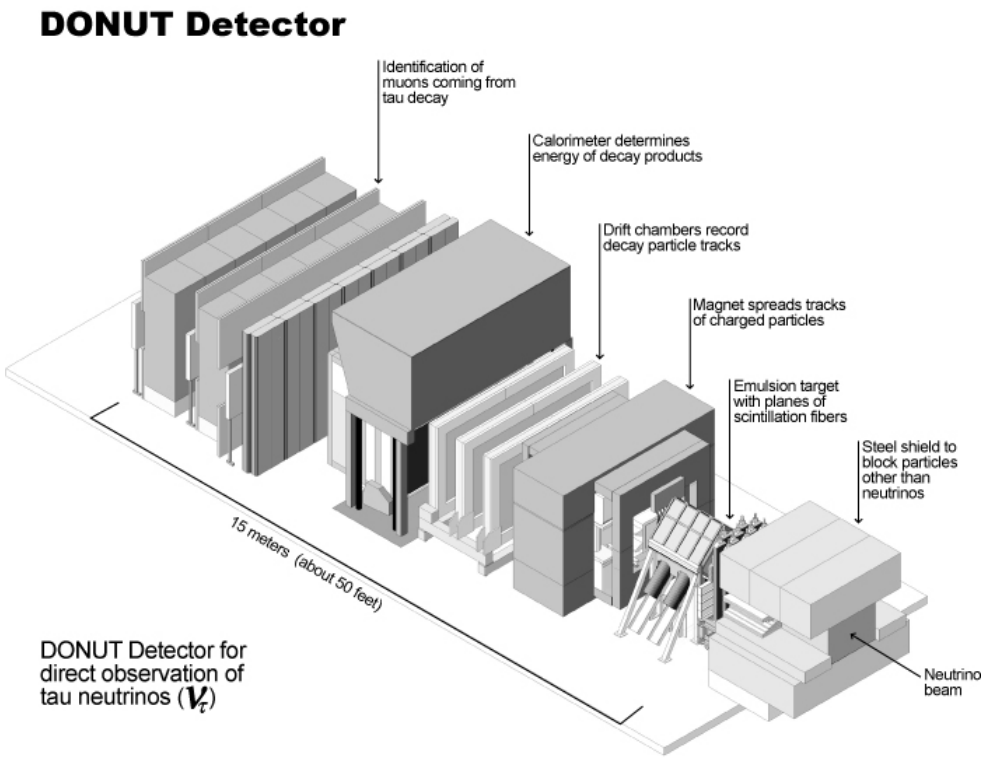

Figure 11.2: DONUT Detector Setup (neutrino beam entering from right)

Chapter 12

Neutrino Number Constraints

In this section, we elucidate the methodologies by which experimental and observational data impose stringent constraints on the number of ***active*** neutrino species. The predictions of Big Bang Nucleosynthesis, which critically depend on the relativistic energy density present in the early universe, are sensitive to the effective number of neutrino species. Moreover, the precision measurement of the Z boson decay width, enables the determination of the invisible decay modes of the Z boson, which are predominantly attributable to neutrino-antineutrino pairs. Collectively, these independent lines of evidence converge on the inference that only three active neutrino species exist, thereby aligning with the expectations of the Standard Model.

12.1 Big Bang Nucleosynthesis (BBN)

Cosmological Framework and Energy Density: Within the framework of the early universe, the total energy density is predominantly determined by relativistic particles. In this regime, the total effective number of relativistic degrees of freedom is given by

$$g_\star(T) = g_\star^{\text{th}}(T) + g_\star^{\text{dec}}(T), \tag{12.1}$$

which contributes to the energy density via

$$\rho(T) = g_\star(T)\frac{\pi^2}{30}T^4. \tag{12.2}$$

where $g_\star^{\text{th}}(T)/g_\star^{\text{dec}}(T)$ is the d.o.f for particles in thermal equilibrium/decoupled, resp. The particle content of the Standard Model (SM) allows for a precise determination of the evolution of $g_\star(T)$ as the universe expands and cools.

Temperature Evolution and Neutrino Decoupling: The evolution of the cosmic temperature is governed by the conservation of entropy. In particular, the temperature T scales with the entropy degrees of freedom $g_{\star S}(T)$ and the scale factor a as follows:

$$T \propto g_{\star S}(T)^{-\frac{1}{3}}a^{-1}. \tag{12.3}$$

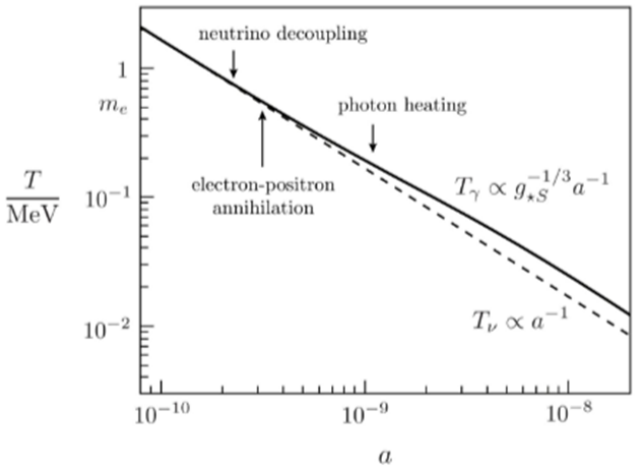

Figure 12.1: Temperature dependence on scale factor during various processes in early Universe

Prior to electron-positron annihilation, and immediately after neutrino decoupling, the effective entropy degrees of freedom are given by

$$g_{\star S}^{\mathrm{th}}(T_+) = 2 + \frac{7}{8}(2+2) = \frac{11}{2}, \tag{12.4}$$

reflecting the contributions of photons and the electron-positron pairs. After electron-positron annihilation, only photons remain in thermal equilibrium, so that

$$g_{\star S}^{\mathrm{th}}(T_-) = 2. \tag{12.5}$$

Conservation of entropy then dictates that the neutrino temperature is related to the photon temperature by

$$T_\nu = \left(\frac{g_{\star S}^{\mathrm{th}}(T_-)}{g_{\star S}^{\mathrm{th}}(T_+)}\right)^{\frac{1}{3}} T_\gamma = \left(\frac{4}{11}\right)^{\frac{1}{3}} T_\gamma. \tag{12.6}$$

Effective Number of Neutrino Species: The total radiation energy density, incorporating the contribution of neutrinos, is expressed as

$$\rho_r = \rho_\gamma \left(1 + \frac{7}{8}\left(\frac{4}{11}\right)^{\frac{4}{3}} N_{\mathrm{eff}}\right). \tag{12.7}$$

In the idealized case of instantaneous neutrino decoupling, the effective number N_{eff} would simply count the number of light, active neutrino species. Thus the 2 processes

$$n + \nu_e \leftrightarrow p + e^- \qquad\qquad n + e^+ \leftrightarrow p + \bar{\nu}_e. \tag{12.8}$$

kept the ratio of neutrons to protons in thermal equilibrium in the early universe as long as the reaction rate $\Gamma \sim G_F^2 T^5$ was larger than the expansion rate (Hubble parameter) $H \sim 1.66\sqrt{g*}T^2/M_P$. H^2 is proportional to the energy density $\rho = g_* \frac{\pi^2 T^4}{30}$, where $g_* \equiv g_B + \frac{7}{8} g_F$, and g_B, g_F are the number of relativistic bosonic and fermionic degrees of freedom in equilibrium at

temperature T [2]. The equilibrium was maintained until the freezeout temperature

$$T_f \sim \left(\frac{\sqrt{g_*}}{G_F^2 M_P}\right)^{1/3} = \mathcal{O}(\text{few MeV}) \tag{12.9}$$

when $\Gamma \sim H$, at which time the n/p ratio was frozen at the value

$$\exp\left(-\frac{m_n - m_p}{T_f}\right) \tag{12.10}$$

except for neutron decay, and most of the neutrons were eventually incorporated into ^{4}He. Thus the abundance of ^{4}He relative to H gives T_F which in turn reveals $N_{\text{eff}}^{\text{SM}} = 3.046$ through $g*$. The slight deviation of $N_{\text{eff}}^{\text{SM}}$ from 3 is due to the non-instantaneous decoupling, and can be reconciled using a more complete treatment of neutrino transport.

Observational Techniques and Their Role in Validating BBN: Observations of low-metallicity H II regions provide a reliable estimate of the primordial ^{4}He abundance, while high-resolution spectroscopic measurements of distant quasar absorption lines yield the deuterium abundance. These observed abundances are then compared to the predictions of BBN models that incorporate the Standard Model particle content. Since any additional relativistic species—such as extra active neutrinos—would alter the expansion rate of the universe and consequently affect the nuclear reaction rates during BBN, the precise match between theoretical predictions and observational data serves as a strong validation of the inferred value of N_{eff}. Specifically, the excellent agreement between the predicted light element abundances and the observed values strongly supports the conclusion that only three active neutrino species exist, in accord with the Standard Model.

12.2 Z Boson Decay and Number of Neutrino Species

The invisible decay width of the Z boson is given by:

$$\Gamma(\text{inv}) = \Gamma_Z - \Gamma(\text{had}) - \sum_i \Gamma(\ell_i \bar{\ell}_i) \tag{12.11}$$

where Γ_Z is the total decay width of the Z boson, $\Gamma(\text{had})$ is the partial width to hadrons, and the sum represents the partial widths into charged lepton-antilepton pairs ($\ell_i \bar{\ell}_i$ for $i = e, \mu, \tau$).

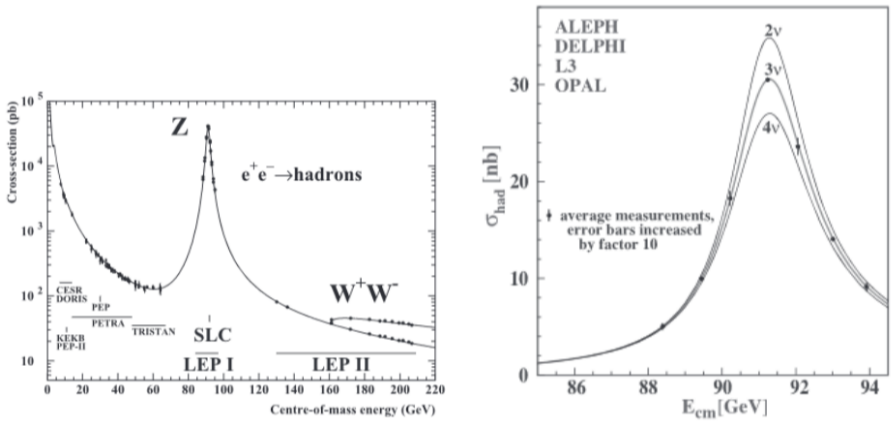

Figure 12.2: Left: The $e^+e^- \to$ hadrons cross-section as a function of the center-of-mass energy shows a prominent resonance at the Z boson mass, indicating the production and decay of Z bosons. Right: The hadronic cross-section σ_{had} around the Z resonance measured by ALEPH, DELPHI, L3, and OPAL experiments at LEP. The curves correspond to different assumptions on the number of neutrino species. The data best matches the prediction for 3 neutrino species.

Assuming the invisible decays of the Z are only to neutrinos, we relate the invisible width to the number of light neutrino species as:

$$\Gamma(\text{inv}) = (3 + \Delta N_\nu)\Gamma(\nu\bar{\nu}) \tag{12.12}$$

where ΔN_ν parametrizes any deviation from the Standard Model prediction of three light neutrino flavors. The best fit on the data gives $3 + \Delta N_\nu = 2.992 \pm 0.007$.

12.3 Sterile Neutrinos?

A set of experimental observations, collectively referred to as the *short baseline anomalies*, have sparked significant interest in the neutrino physics community. These anomalies arise in data sets that are sensitive to small values of the ratio L/E (baseline length over energy), which are too small for the known neutrino oscillation frequencies to significantly manifest. Despite this, unexpected neutrino behavior has been observed in several experiments.

The anomalies can be grouped into three general categories:

- **Appearance of electron neutrinos:** Experiments such as LSND and MiniBooNE have reported a signal consistent with $\nu_\mu \to \nu_e$ appearance at short baselines, beyond what is predicted by the three-neutrino paradigm.
- **Disappearance of electron neutrinos:** Radioactive source experiments, designed to detect ν_e via known interactions, have observed fewer events than expected, suggesting possible $\nu_e \to \nu_{\text{other}}$ disappearance.
- **Disappearance of electron antineutrinos:** Reactor experiments (France, Daya Bay) have similarly shown a deficit in $\bar{\nu}_e$ flux compared to predictions, pointing towards possible

$\bar{\nu}_e \to \bar{\nu}_{\text{other}}$ transitions. [6]

Although none of these anomalies are individually conclusive, and their combination does not yield a universally accepted solution, they are also not easily dismissed as mere statistical fluctuations. These persistent discrepancies may indicate physics beyond the Standard Model.

One possibility is the existence of a fourth, *sterile* neutrino — a neutrino species that does not interact via the weak force and hence is undetectable by conventional means. Such a particle could explain the observed anomalies via mixing with the active neutrinos.

12.4 The STEREO experiment

This was designed to test the hypothesis of oscillations of electron antineutrinos into sterile neutrino states. This was particularly motivated by the Reactor Antineutrino Anomaly (RAA), which observed a deficit in detected $\bar{\nu}_e$ flux compared to theoretical predictions.

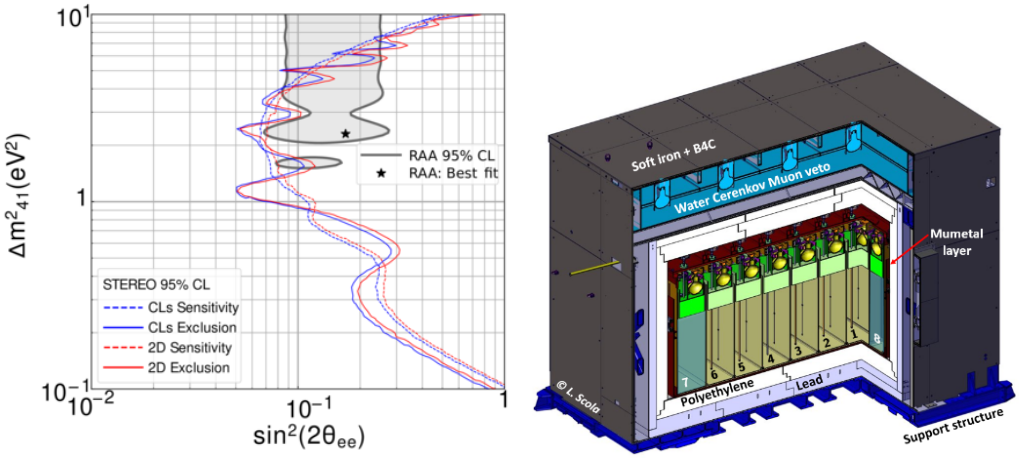

(a) (b)

Figure 12.3: (a)Final results excluding RAA parameter space (b) Schematic of the STEREO experiment

The detector consists of an organic liquid scintillator doped with gadolinium (Gd), which allows for the detection of inverse beta decay reactions:

$$\bar{\nu}_e + p \to n + e^+. \tag{12.13}$$

The positron (e^+) produces prompt scintillation light upon annihilation, while the neutron is captured by gadolinium after thermalization, producing a delayed secondary signal. This coincidence signature enables clean identification of neutrino interactions.

The STEREO detector is segmented into six cells arranged along the axis pointing to the reactor core. These segments allow for simultaneous measurement of the energy spectrum of incoming neutrinos at different baselines, covering a range of about 2 meters. This distance

corresponds to the expected oscillation wavelength for a sterile neutrino with mass-squared differences in the range $\Delta m^2 \sim 1$ eV^2.

The experiment's final results excluded most of the parameter space that could account for the Reactor Antineutrino Anomaly at a 90% confidence level, placing significant constraints on the existence of light sterile neutrinos.

Chapter 13

Neutrino Oscillation Experiments

13.1 Solar Neutrinos

Neutrinos (ν_e) are produced by fusion reactions in main sequence stars by the *pp* and *CNO* chains, which ultimately lead to $4p \rightarrow \alpha + 2e^+ + 2\nu_e$. The *standard solar model* (SSM) [7], which is well tested and constrained by helioseismology and other solar observations, and by the properties of other stars, is dominated by the *pp* chain, which produce low energy but high intensity neutrinos. The most important reactions are

$$p + p \rightarrow D + e^+ + \nu_e, \quad D + p \rightarrow {}^3He + \gamma, \quad 2\ {}^3He \rightarrow \alpha + 2p. \tag{13.1}$$

Though rare, the Sun also produces high energy neutrinos through

$${}^3He + \alpha \rightarrow {}^7Be + \gamma, \quad {}^7Be + e^- \rightarrow {}^7Li + \nu_e, \tag{13.2}$$

$${}^7Be + p \rightarrow {}^8B + \gamma, \quad {}^8B \rightarrow {}^8Be^* + e^+ + \nu_e, \tag{13.3}$$

which leads to the ${}^8B$ neutrinos. These are insignificant numerically, but because of their much higher energy are easiest to detect. The flux of *pp* neutrinos is well constrained by the observed solar luminosity, but the predicted ${}^7Be$ and (especially) ${}^8B$ fluxes are much more uncertain because of their strong dependence on the temperature of the solar core, low energy nuclear cross sections, and the solar composition.

The first hints of neutrino oscillation were provided by solar neutrino experiments, which consistently measured a deficit in the expected flux of electron neutrinos (ν_e) originating from the Sun.

13.2 Early Experiments: Homestake and Kamiokande

One of the pioneering experiments was the **Homestake experiment**, which employed a radiochemical method using chlorine:

$$^{37}\mathrm{Cl} + \nu_e \rightarrow e^- + {}^{37}\mathrm{Ar}$$

with a threshold energy of 814 keV (sensitive to only high-energy neutrinos). The experiment used 10^5 gallons of water duped Cl, and Ar atoms were extracted using a Helium displacement procedure. This experiment detected only approximately 33% of the solar ν_e flux predicted by the Standard Solar Model (SSM). [8]

Subsequent efforts, such as the **Kamiokande** and **Super-Kamiokande** experiments in Japan, utilized large water Cherenkov detectors sensitive to the elastic scattering process:

Charged Current (CC):

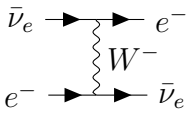

Neutral Current (NC):

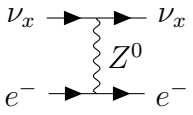

Figure 13.1: Feynman diagrams for solar (anti)neutrino scattering off electrons via the charged and neutral current interactions.

This interaction allows for detection of all neutrino flavors, with electron neutrinos participating via both charged current (CC) and neutral current (NC) interactions, and other flavors only through NC. Despite this inclusive sensitivity, these experiments reported a flux corresponding to only $\sim 50\%$ of the SSM prediction.

Two possible explanations emerged:

- Incomplete understanding of solar astrophysics.
- The possibility of neutrino flavor transformation, i.e., **neutrino oscillation**.

13.3 Gallium Experiments: Sensitivity to Low-Energy ν_e

To distinguish between these hypotheses, a new generation of experiments based on **Gallium** targets was undertaken, exploiting the reaction:

$$\nu_e + {}^{71}\mathrm{Ga} \rightarrow e^- + {}^{71}\mathrm{Ge}$$

This interaction has a low energy threshold of 233 keV, making it sensitive to the dominant low-energy *pp* neutrinos emitted by the Sun.

If the measured flux in these experiments matched the reduced ^{8}B flux observed in Kamiokande, it would support the neutrino oscillation hypothesis. Conversely, agreement with the full SSM prediction would point to unknown astrophysical mechanisms.

Experiments such as **GALLEX**, **GNO** (Italy), and **SAGE** (Russia) consistently measured solar neutrino fluxes of approximately $\gtrsim 50\%$ of the SSM expectation. This result effectively ruled out deficiencies in solar modeling and strongly favored neutrino oscillations as the source of the observed flux suppression.

13.4 Definitive Evidence: The Sudbury Neutrino Observatory

The conclusive resolution of the solar neutrino problem came from the **Sudbury Neutrino Observatory** (SNO), which utilized heavy water (D_2O) as a detection medium. The central element was 1000 tonnes of heavy water ($\gtrsim 99.5\%$ isotopically pure), and was surrounded by 9438 20-cm diameter photomultiplier tubes (PMTs). Deuterium nuclei (d) are sensitive to all neutrino flavors and enable discrimination among them via distinct interaction channels:

$$\nu_e + d \to p + p + e^- \quad \text{(Charged Current)} \tag{13.4}$$

$$\nu_x + e^- \to \nu_x + e^- \quad \text{(Elastic Scattering)} \tag{13.5}$$

$$\nu_x + d \to p + n + \nu_x \quad \text{(Neutral Current)} \tag{13.6}$$

By comparing the rates of these interactions, SNO demonstrated that the total solar neutrino flux (from all flavors) agreed with SSM predictions, while the electron neutrino component alone was deficient. This provided unambiguous, model-independent evidence for neutrino flavor transformation, thereby confirming the phenomenon of neutrino oscillation. [9]

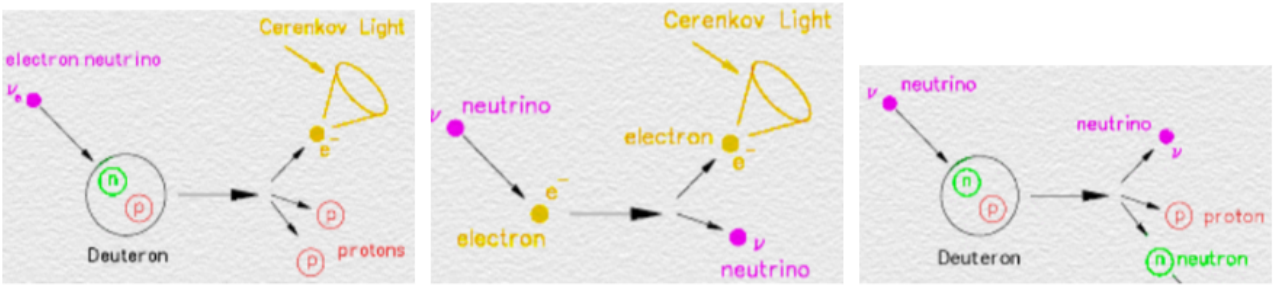

Figure 13.2: Illustration of SNO detection processes for different neutrino flavors.

13.5 Atmospheric Neutrinos

Primary cosmic rays, predominantly protons (p^+), interact with nuclei in the upper atmosphere, producing pions and muons. These decay chains result in the production of both electron and muon neutrinos:

$$\pi^+ \to \mu^+ + \nu_\mu \quad \text{followed by} \quad \mu^+ \to e^+ + \nu_e + \bar{\nu}_\mu \tag{13.7}$$

As shown in Figure 8, neutrinos are generated at different points in the atmosphere and can travel varying path lengths before reaching the detector, depending on their direction (i.e., zenith angle).

Oscillations of neutrinos were firmly established by measuring the ν_μ/ν_e flux ratio coming from the atmosphere. While the expected value without oscillations is approximately 2, the observed value was closer to 1.2. This discrepancy, with zenith-angle flux asymmetries, provided unambiguous evidence for neutrino oscillations.

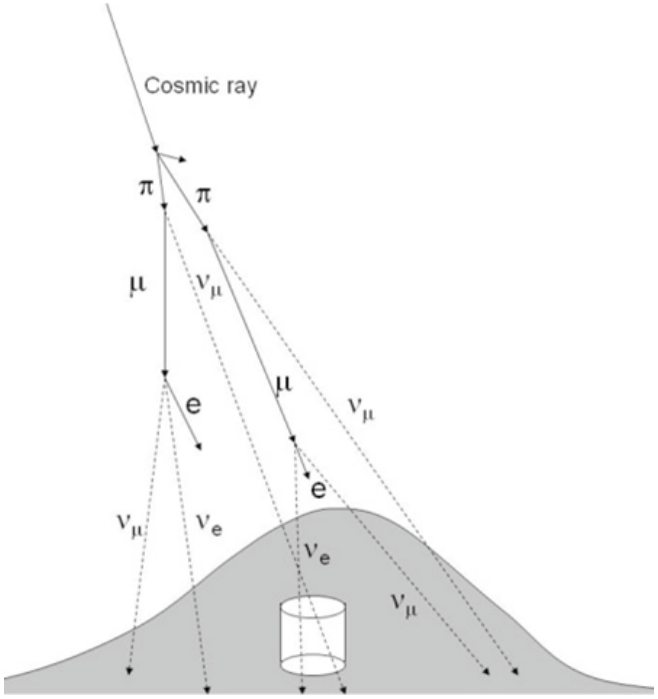

Figure 13.3: Schematic of atmospheric neutrino production and detection.

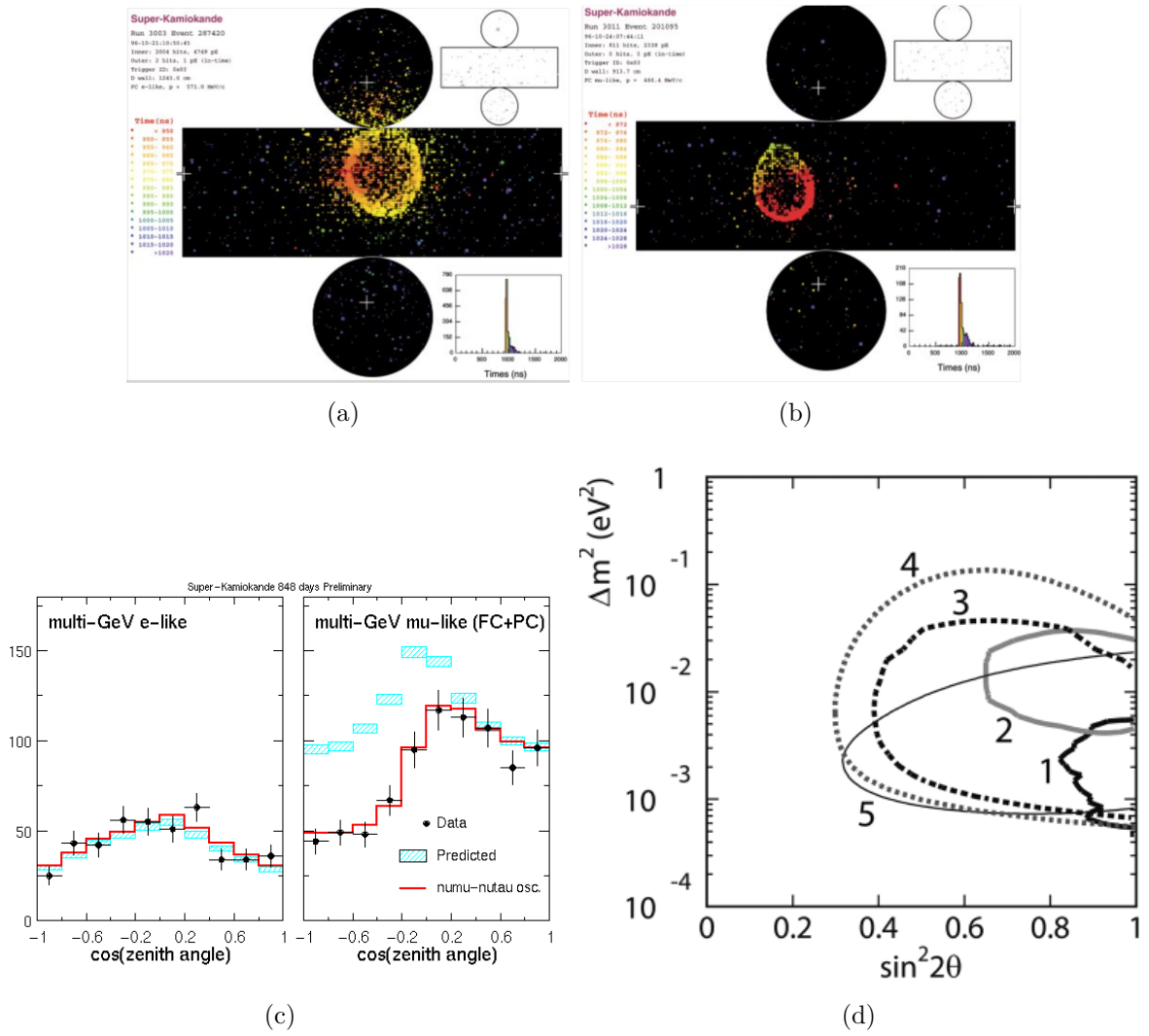

Figure 13.4: (a)Super-Kamiokande PMT signals for e-like events (b)Super-Kamiokande PMT signals for μ-like events (c)Observed hits vs zenith angle ($cos\theta$) resp. (d)Allowed parameter regions of $\nu_\mu \rightarrow \nu_\tau$ oscillations from Super-Kamiokande and Kamiokande shown at the Neutrino'98 conference.

These measurements were taken with the Super-KamioKande experiment, with a fiducial volume of 22.5 kilotonnes and approximately 11.000 PMTs, supplemented by timing arrays that recorded the arrival times of signals Figure 9 shows examples of photomultiplier tube signals and the interpreted measurements. Pattern recognition algorithms are able to easily differentiate between an e^- and μ^- event thanks to the large spread of the e-like signal, caused by EM showers (pair-production and bremsstrahlung).

From Figure 9(c), it is clear that a defecit of upward-going μ-like events was observed. The statistical significance was more than 6σ, implying that this is not a statistical fluctuation. This implied some physical mechanism to reduce the number of ν_μ interactions for neutrinos that traveled more than several hundred km. On the other hand, the zenith angle distribution for e-like events did not show any statistically significant up-down asymmetry. This suggested that the ν_e events were detected as expected independent of the neutrino flight length. Essentially, electron-neutrinos do not oscillate as far as the flight length is less than the diameter of the

Earth. It was concluded from these plots that muon-neutrinos oscillate to other types of neutrinos,now known to be tau-neutrinos. Furthermore, the zenith-angle distributions for upward going muons, produced by very high energy atmospheric neutrino interactions in the rock below the Super-Kamiokande detector, showed a deviation from the non-oscillated Monte Carlo prediction; another indication of oscillations. The data were analyzed assuming $\nu_\mu \rightarrow \nu_\tau$ neutrino oscillations, and allowed parameter contours from various data-sets of Super-Kamiokande and Kamiokande (Fig 9(d)) indicated that the data were consistently explained by neutrino oscillations.

Chapter 14

Neutrinoless Double-β Decay

A promising method to probe the Majorana nature of neutrinos is the search for neutrino-less double β-decay. In some radioactive isotopes, the single β-decay process is energetically forbidden; however, these nuclei can undergo double β-decay. In the neutrinoless mode, the absence of emitted neutrinos would indicate that neutrinos are Majorana particles—i.e., their own antiparticles.

Figure 10 displays the Feynman diagrams and measured vs. expected histograms in case of double β-decays. Since the e^{-}s carry away all the energy during a neutrino-less double beta decay, we expect to see a spike in the histogram at the Q-value (decay energy). However, due to extremely long (theoretical) lifetimes of the reaction ($\ln T^{0\nu}_{\beta\beta} \gtrsim 22$, where $T^{0\nu}_{\beta\beta}$ in yrs), noise becomes a significant deterrant. [10] Experiments such as KamLAND-ZEN and NEMO-3 have been at the forefront of these searches. The KamLAND-ZEN experiment employs a xenon-loaded liquid scintillator to search for neutrinoless double β-decay in ^{136}Xe, while the NEMO-3 experiment utilizes a combination of tracking and calorimetry to study various $\beta\beta$-decaying isotopes. Recent updates from these experiments have set increasingly stringent limits on the effective Majorana neutrino mass, although a conclusive signal remains elusive.

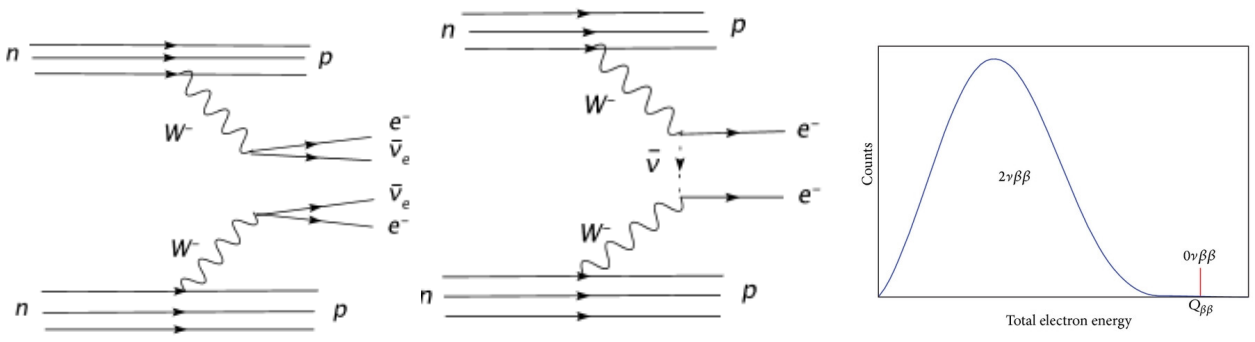

(a) (b) (c)

Figure 14.1: (a)Super-Kamiokande PMT signals for e-like events (b)Super-Kamiokande PMT signals for μ-like events (c)Observed hits vs zenith angle ($cos\theta$) resp. (d)Allowed parameter regions of $\nu_\mu \to \nu_\tau$ oscillations from Super-Kamiokande and Kamiokande shown at the Neutrino'98 conference.

Part V

Conclusions

Chapter 15

A Final Word

Throughout the report, a few interesting phenomena of neutrinos were examined, both from a theoretical and experimental standpoint. Though very much a part of the Standard Model, neutrino physics provides a unique window into physics beyond the Standard Model. The observed neutrino masses, oscillations, and potential signals of lepton number violation—such as neutrinoless double β-decay strongly indicate the need for new theoretical frameworks. These phenomena not only challenge the conventional SM paradigm but also offer promising avenues for exploring grand unification, dark matter, and leptogenesis.

Bibliography

[1] C. P. Burgess and G. D. Moore. *The standard model: A primer*. Cambridge University Press, Dec. 2006. ISBN: 978-0-511-25485-7, 978-1-107-40426-7, 978-0-521-86036-9.

[2] Paul Langacker. *The Standard Model and Beyond*. 2nd ed. CRC Press, 2017. DOI: 10.1201/b22175. URL: https://doi.org/10.1201/b22175.

[3] C. L. Cowan et al. "Detection of the Free Neutrino: a Confirmation". In: *Science* 124.3212 (1956), pp. 103–104. DOI: 10.1126/science.124.3212.103. eprint: https://www.science.org/doi/pdf/10.1126/science.124.3212.103. URL: https://www.science.org/doi/abs/10.1126/science.124.3212.103.

[4] Ivan V. Anicin. *The Neutrino - Its Past, Present and Future*. 2005. arXiv: physics/0503172 [physics.hist-ph]. URL: https://arxiv.org/abs/physics/0503172.

[5] K. Kodama et al. "Final tau-neutrino results from the DONuT experiment". In: 78.5, 052002 (Sept. 2008), p. 052002. DOI: 10.1103/PhysRevD.78.052002. arXiv: 0711.0728 [hep-ex].

[6] G. Mention et al. "The Reactor Antineutrino Anomaly". In: *Phys. Rev. D* 83 (2011), p. 073006. DOI: 10.1103/PhysRevD.83.073006. arXiv: 1101.2755 [hep-ex].

[7] Wick C Haxton, RG Hamish Robertson, and Aldo M Serenelli. "Solar neutrinos: status and prospects". In: *Annual Review of Astronomy and Astrophysics* 51.1 (2013), pp. 21–61.

[8] Bruce T. Cleveland et al. "Measurement of the Solar Electron Neutrino Flux with the Homestake Chlorine Detector". In: *The Astrophysical Journal* 496.1 (Mar. 1998), p. 505. DOI: 10.1086/305343. URL: https://dx.doi.org/10.1086/305343.

[9] A. Bellerive et al. "The Sudbury Neutrino Observatory". In: *Nucl. Phys. B* 908 (2016), pp. 30–51. DOI: 10.1016/j.nuclphysb.2016.04.035. arXiv: 1602.02469 [nucl-ex].

[10] S. M. Bilenky and C. Giunti. "Neutrinoless Double-Beta Decay: a Probe of Physics Beyond the Standard Model". In: *Int. J. Mod. Phys. A* 30.04n05 (2015), p. 1530001. DOI: 10.1142/S0217751X1530001X. arXiv: 1411.4791 [hep-ph].